Atmos. Chem. Phys. Discuss., 12, 20311–20350, 2012
www.atmos-chem-phys-discuss.net/12/20311/2012/
doi:10.5194/acpd-12-20311-2012

Atmospheric Chemistry and Physics Discussions

Formation of anthropogenic secondary organic aerosol (SOA) and its influence on biogenic SOA properties

E. U. Emanuelsson[1], M. Hallquist[1], K. Kristensen[2], M. Glasius[2], B. Bohn[3], H. Fuchs[3], B. Kammer[3], A. Kiendler-Scharr[3], S. Nehr[3], F. Rubach[3], R. Tillmann[3], A. Wahner[3], H.-C. Wu[3], and Th. F. Mentel[3]

[1]Department of Chemistry and Molecular Biology, University of Gothenburg, 412 96 Göteborg, Sweden
[2]Department of Chemistry, Aarhus University, 8000 Aarhus, Denmark
[3]Institut für Energie- und Klimaforschung: Troposphäre (IEK-8), Forschungszentrum Jülich, 52 428 Jülich, Germany

Received: 11 July 2012 – Accepted: 26 July 2012 – Published: 14 August 2012

Correspondence to: Th. F. Mentel (t.mentel@fz-juelich.de)

Published by Copernicus Publications on behalf of the European Geosciences Union.

Abstract

Secondary organic aerosol (SOA) formation from mixed anthropogenic and biogenic precursors has been studied exposing reaction mixtures to natural sunlight in the SAPHIR chamber in Jülich, Germany. Several experiments with exclusively anthropogenic precursors were performed to establish a relationship between yield and organic aerosol mass loading for the atmospheric relevant range of aerosol loads of 0.01 to 10 $\mu g\,m^{-3}$. The yields (0.5–9 %) were comparable to previous data and further used for the detailed evaluation of the mixed biogenic and anthropogenic experiments. For the mixed experiments a number of different oxidation schemes were addressed. The reactivity, the sequence of addition, and the amount of the precursors influenced the SOA properties. Monoterpene oxidation products, including carboxylic acids and dimer esters were identified in the aged aerosol at levels comparable to ambient air. OH radicals were measured by Laser Induced Fluorescence, which allowed for establishing relations of aerosol properties and composition to the experimental OH dose. Furthermore, the OH measurements in combination with the derived yields for anthropogenic SOA enabled application of a simplified model to calculate the chemical turnover of the anthropogenic precursor and corresponding anthropogenic contribution to the mixed aerosol. The estimated anthropogenic contributions were ranging from small (≈ 8 %) up to significant fraction (> 50 %) providing a suitable range to study the effect of aerosol composition on the aerosol volatility (volume fraction remaining at 343 K: 0.86–0.94). The anthropogenic aerosol had higher oxygen to carbon ratio O/C and was less volatile than the biogenic fraction. However, in order to produce significant amount of anthropogenic SOA the reaction mixtures needed a higher OH dose that also increased O/C and provided a less volatile aerosol. A strong positive correlation was found between changes in volatility and O/C with the exception during dark hours where the SOA volatility decreased while O/C did not change significantly. This change in volatility under dark conditions is likely due to chemical or morphological changes not affecting O/C.

ACPD

12, 20311–20350, 2012

1 Introduction

Formation of atmospheric secondary organic aerosol (SOA) from gas-phase precursors has received considerable attention during the last decade (Hallquist et al., 2009; Jimenez et al., 2009; De Gouw and Jimenez, 2009; Kroll and Seinfeld, 2008). Secondary organic aerosol components impact the Earth climate by supporting the formation of new particles, which increases the number density, and by condensation onto pre-existing particles, which increases both mass and size. Moreover, SOA formation and transformation by atmospheric processes influence the physicochemical properties of atmospheric aerosols. Depending on location, time and specific source regions, SOA can be produced from both anthropogenic and biogenic volatile organic compounds (VOC). Globally the production of biogenic SOA (BSOA) dominates over the anthropogenic (ASOA) with estimated fluxes of 88 and 10 $\mathrm{Tg\,C\,yr^{-1}}$, respectively (Hallquist et al., 2009). As discussed by Hallquist et al. (2009) there are large uncertainties but all estimates indicate the production of BSOA to be significantly larger than ASOA (Spracklen et al., 2011; Kanakidou et al., 2005; Heald et al., 2010; Goldstein and Galbally, 2007). Locally and regionally however, the ASOA can supersede the BSOA (e.g. Fushimi et al., 2011; Steinbrecher et al., 2000; Aiken et al., 2009). The SOA formation mechanisms are complex and even though we nowadays have a detailed chemical knowledge on the degradation of most VOC, a large part of the SOA formation and ageing is still unclear as well as understanding multi-component systems. There are several field observations where SOA has been attributed to originate from both biogenic and anthropogenic sources and it seems that anthropogenic activities enhance BSOA abundance (e.g. Aiken et al., 2009; Carlton et al., 2010; de Gouw et al., 2005, 2008; Hu et al., 2008; Shantz et al., 2004; Spracklen et al., 2011; Szidat et al., 2006, 2009).

Several studies have recently stressed the potential of anthropogenic biogenic interactions to be of importance for SOA (Spracklen et al., 2011; Hoyle et al., 2011; Glasius et al., 2011; Galloway et al., 2011; Kautzman et al., 2010). There are several

ACPD
12, 20311–20350, 2012

potential ways of interactions, both directly by gas-aerosol chemistry and physics, and indirectly by anthropogenic influence on biogenic source strengths. In the context of the present study the chemistry of VOC from anthropogenic (AVOC) and biogenic (BVOC) compounds will be covered. This has also been the main focus of the recent laboratory study of Hildebrandt et al., 2011 and is partly covered in a number of other studies during the last years (Jaoui et al., 2008; Lambe et al., 2011; Hildebrandt et al., 2011; Derwent et al., 2010). Hildebrandt et al. found that ABSOA derived from mixtures of AVOC and BVOC can be treated as ideal mixtures. The yields can be parameterised applying the assumption of a common organic phase for partitioning. In the atmosphere there are a number of interesting issues regarding SOA formation from mixed air masses where typical anthropogenic precursors behave differently compared to biogenic precursors. Typical anthropogenic SOA precursors (AVOC) are aromatic hydrocarbons whereas typical biogenic precursors (BVOC) are terpenoids. As shown in Table 1 benzene, toluene, and p-xylene (here representing AVOC) react slower with OH radicals than the unsaturated monoterpenes α-pinene and limonene (here representing BVOC). Moreover, monoterpenes can also be oxidized by ozone and NO_3 enabling SOA production also during dark conditions. In order to elucidate this further, chamber studies were conducted here to mimic a few selected scenarios where anthropogenic and biogenic precursors were oxidised and aged both together and separately. In addition to characterisation of SOA composition by aerosol mass spectrometry, filter samples were analysed to achieve insight into chemical composition related atmospheric persistence (volatility).

2 Experimental

The oxidation of the VOC precursors and the following SOA formation took place in the outdoor atmosphere simulation chamber SAPHIR located on the campus of Forschungszentrum Jülich. SAPHIR is a double-wall Teflon chamber of cylindrical shape of a volume of 270 m^3 and has previously been described (Rohrer et al.,

ACPD
12, 20311–20350, 2012

2005; Bohn et al., 2005). SAPHIR is operated with synthetic air (Linde Lipur, purity 99.9999 %) and kept under a slight overpressure of about 50 Pa. Characterization of gas phase and SOA particles were performed with a number of instruments (see below). A continuous flow of synthetic air of 7–9 $m^3 h^{-1}$ maintained the chamber overpressure and compensated for the sampling by the various instruments. This flow causes dilution of the reaction mixture with clean air. The synthetic air is also used to permanently flush the space between the inner and the outer Teflon wall. This and the overpressure of the chamber serve to prevent intrusion of contaminants into the chamber. The chamber is protected by a louvre system, which is either opened to simulate daylight conditions, exposing the reaction mixtures in the chamber to natural sun light or closed to simulate processes in the dark. A fan ensured mixing of trace gases within minutes, but reduced aerosol lifetime to about 6 h.

In this work 17 yield experiments listed in Table 1 were performed with individual aromatic (anthropopenic) precursors (benzene, toluene, p-xylene, mesitylene, hexamethylbenzene or p-cymene (biogenic)) producing the ASOA at low NO_x ($\approx$ 1 ppb) and high NO_x ($\approx$ 10 ppb) conditions. ASOA yields were determined from these experiments. A 1 : 1 mixture of α-pinene and limonene served as biogenic precursors during other experiments. Three of the ASOA experiments and four mixed experiments (ABSOA) with biogenic and anthropogenic precursors were analysed in detail and the experimental procedures for these experiments are illustrated in Fig. 1. In ABSOA 10/6, the BVOC mixture was added initially and photo-oxidised for 2.5 h before the AVOC (toluene) was added and the mixture was further exposed to sunlight for 3.5 h prior to filter sampling. In ABSOA 11-12/6 the AVOC was added first and oxidised in sunlight for 5.75 h before the BVOC was added in the dark and the mixture was exposed to ozone overnight. The ozone was initially about 20 ppb and originated from the previous photochemistry. Before the filter sampling on the subsequent 2nd day the mixture was exposed to sunlight for another 4 h. ABSOA 14-15/6 is the analogue to ABSOA 11-12/6 but using xylene instead of toluene as ASOA precursor. During exp. 11/6 the mixing fan failed at 13:20 h leading to reduced particles losses during filter sampling and the

ACPD
12, 20311–20350, 2012

subsequent ABSOA part of the experiment. For the fourth ABSOA experiment (22/6) BVOC and AVOC was added simultaneously and exposed for photo-oxidation during 6.3 h. The experiments 13/6 and 18–19/6 illustrate pure ASOA (toluene) and BSOA (α-pinene) cases respectively.

The SAPHIR chamber is equipped with a suite of instruments. For this study several gas concentrations like O_3, NO and NO_2 were monitored, as were temperature and relative humidity. The actinic flux and the according photolysis frequencies were provided from measurements with a spectral radiometer (Bohn et al., 2005). In this study we employed PTR-MS to monitor the concentrations of the VOC (Jordan et al., 2009). Particle number and number size distributions were measured by condensation particle counter (UWCPC, TSI3786) and a scanning mobility particle sizer (SMPS, TSI3081/TSI3786).

Laser Induced Fluorescence (LIF) was applied to measure hydroxyl radicals (OH). The LIF instrument is described in detail by Fuchs et al., 2012. We calculated the OH dose in order to better compare experiments at different conditions. The OH dose is the integral of the OH concentration over time and gives the cumulated OH concentrations to which gases, vapours and particles were exposed at a given time of the experiment. One hour exposure to typical atmospheric OH concentrations of 2×10^6 cm^{-3} results in an OH dose of 7.2×10^9 cm^{-3} s.

A high-resolution time-of-flight aerosol mass spectrometer (HR-ToF-AMS, Aerodyne Research Inc., DeCarlo et al., 2006) was used to measure the chemical composition of the SOA. The particles enter the instrument through an aerodynamic lens that reduces gas phase by about 10^7 with respect to the particle concentration, so that only particle composition is detected, except for the main components of air; N_2, O_2, CO_2 and H_2O vapour. A tungsten oven at 600 °C flash-vaporizes the particles under vacuum. The vapours are ionized by 70 eV electron impact (EI), and the resulting ions are detected by means of a time-of-flight mass spectrometer applying either a high-sensitivity mode (V-mode) or a high-mass resolution mode (W-mode). In this study we made use of the

ACPD
12, 20311–20350, 2012

so-called MS mode, where ion signals are integrated over all particle sizes, thus the overall composition of the SOA is determined.

To characterize the degree of oxidation of the particles, two approaches were applied. The O/C ratio was derived by elemental analysis of mass spectra obtained in the high-mass resolution W-mode as described by Aiken et al. (2007, 2008). As a proxy for O/C ratio that can be measured with higher signal to noise ratio, the ratio f44 was also determined from high sensitivity V-mode data. The ratio f44 is defined as the ratio of mass concentration of CO_2^+ ions ($m/z = 44$ Th) to the signal of all particulate organics measured by AMS. Using all data where the organic mass loading was at least $0.5\,\mu g\,m^{-3}$, we find a linear relationship between O/C and f44 with a slope = 3.3 ± 0.04, an intercept = 0.09 ± 0.004 and $R^2 = 0.9094$. In a similar way as f44 characterizes the presence of carboxylic acids, f43 ($m/z = 43$ Th divided by all organics) characterizes the presence of less oxidized, carbonyl like material.

Corrections for the (minor) influence of gaseous components preceded the calculation of the O/C ratio, f44 and f43. Chamber air contains CO_2 and water vapour and both gas phase species contribute to the mass spectra. The contribution of gas-phase CO_2 to *m/z* 44 and water vapour to *m/z* 18 was inferred from measurements during periods when no particles were present. The values were subtracted to obtain the particle signals for the elemental analysis (Allan et al., 2004).

A volatility tandem differential mobility analyser (VTDMA) set-up (Jonsson et al., 2007; Salo et al., 2011) was used to determine the thermal characteristics of the organic aerosol particles. The aerosol was sampled from the SAPHIR chamber using 6 mm stainless steel tubing and dried using a Nafion drier (Perma Pure PD100T-12MSS). A narrow particle diameter range was then selected using a Differential Mobility Analyser (DMA) operated in a re-circulating mode. The size selected aerosol was directed through one of the eight temperature controlled paths in an oven unit under laminar flow conditions. Each heated oven consists of a 50 cm stainless steel tube mounted in an aluminium block with a heating element set independently from 298 to 563 K ± 0.1 K. To enable swift changes in evaporative temperatures the sample flow

ACPD
12, 20311–20350, 2012

(0.3 LPM) was switched between the ovens giving a residence time in the heated part of the oven of 2.8 s, calculated assuming plug flow. At the exit of the heated region, the evaporated gas was adsorbed by activated charcoal diffusion scrubbers to prevent re-condensation. The residual aerosol was finally classified using a scanning mobility particle sizer (SMPS). Because of low aerosol concentrations, the initial median particle diameter was selected to dynamically follow the aerosol size distribution and was typically set around 80 nm. From the initial particle mode diameter (D_{Ref}) determined at reference temperature (298 K) and the final particle mode diameter (D_T) after evaporation at an elevated temperature, the Volume Fraction Remaining (VFR_T) was defined as $VFR_T = (D_T/D_{Ref})^3$ assuming spherical particles. This procedure was used to ensure that any change in particle diameter was a result of evaporation in the oven unit and to minimise artefacts such as evaporation in the sampling lines prior the VTDMA (Salo et al., 2011). Thermal characterisation was done repeatedly at several temperatures (from 298 up to 563 K) or the evolution of volatility with time was monitored at a fixed temperature, e.g. VFR_{343K}. An increase in VFR corresponds to a less volatile and more persistent aerosol particle.

At the end of experiment sections filter samples were collected to get detailed insight into the chemical composition of the aerosol particles. The filter samples were taken using a preceding annular denuder coated with resin to remove gaseous species. The PTFE filters (ADVANTEC PTFE, pore size 0.2 µm, Ø 47 mm) were placed in stainless steel housing. Two filters were sampled after each other with a flow of 20 l min^{-1}, 1 h $filter^{-1}$, after the roof was closed at the end of the day. Filters were stored at 253 K prior to analysis. Extraction and analysis of the organic aerosol from the filters followed the method of Kristensen and Glasius (2011) and will only be described briefly here. Samples were extracted in acetonitrile, and the extracts were evaporated to dryness and reconstituted in 200 µl of 0.1 % acetic acid and 3 % acetonitrile in water. All prepared samples were kept at 268 K until analysis. Sample extracts were analysed using a Dionex Ultimate 3000 HPLC system coupled through an electrospray (ESI) inlet to a q-TOF mass spectrometer (microTOFq, Bruker Daltonics GmbH, Bremen, Germany)

ACPD
12, 20311–20350, 2012

operated in negative mode. The HPLC stationary phase was a Waters T3 C18 column (2.1 × 150 mm; 3 µm particle size), while the mobile phase consisted of acetic acid 0.1 % (*v*/*v*) and acetonitrile. Pinonic acid, *cis*-pinic acid, terpenylic acid, diaterpenylic acid acetate (DTAA) and 3-methyl butane tricarboxylic acid (MBTCA) were quantified using authentic standards. Oxidation products from limonene along with dimer esters from α-pinene were quantified using pinonic acid, *cis*-pinic acid and DTAA as surrogate standards. Recovery from spiked filters was 72–88 % for all compounds except MBTCA (55 %). No correction for losses during sample handling was applied. Detection limits were 1.1–3.5 ng m^{-3} and analysis of two unexposed filters showed concentrations close to detection limits.

3 Methods

Aerosol yields from single anthropogenic precursors were determined in experiments with production of ASOA only. The aromatic compounds have two loss terms in the SAPHIR chamber: flush out and reaction with OH. The flush-out rate is very well defined in the chamber as the replenishment flow is measured directly and can in addition be deduced from inert tracers like CO_2 or absolute water concentration. The chemical turnover of the aromatic compounds was determined in seven minute time steps by using the measured concentration drop of the aromatic compound corrected for the loss by flush-out. For some cases we additionally calculated the chemical turnover in a different way, applying the measured OH and AVOC concentrations and the rate coefficient at each time step. In these cases, the sum of chemical loss and flush out deviated at maximum 15 % from the observed total turnover. Particles have additional loss terms in the chamber since they deposit and diffuse to the walls. These losses were estimated assuming that the aerosol mass concentration (C_{OA}) should be constant at long times, in absence of aerosol production after correction for all loss terms. The yield is thus given by the chemical turnover of the aromatic compounds divided by

ACPD
12, 20311–20350, 2012

the loss corrected C_{OA} at the end of the day, i.e. before closing the roof. The error in the yield calculation according to this approach is estimated to ±20 %.

In order to estimate the anthropogenic fraction in the mixed anthropogenic/biogenic ABSOA systems a simple chemical/partitioning model was used. The model inputs were the gas-phase concentrations of OH, the aromatic precursor and the particle mass as observed. We calculated the sum of all products (P_{sum}) formed by the reactions of the aromatics with OH:

$$\text{AVOC} + \text{OH} \rightarrow P_{sum} \quad (1)$$

By using the measured particle mass and the yield function derived from pure ASOA experiments we calculated at each seven minutes time interval the fraction of P_{sum} which supposedly is residing in the particulate phase (PP_{sum}) and in the gas phase (GP_{sum}). This information was used to calculate loss terms for GP_{sum} by flush out and for PP_{sum} by flush out and particle loss. The model thus delivers the amount of particulate aromatic products PP_{sum} and its fractional contribution to the total mixed aerosol. This procedure assumes instantaneous partitioning in order to correct for particle loss during the experiments. The estimated values will be most representative at those times when the chemistry is evolved sufficiently and when the estimated macroscopic yield describes the partitioning of all oxidation products, i.e. at the end of the experiments. This procedure may overestimate the actual loss of P_{sum}, if the dynamically derived PP_{sum} is over-predicted due to slow partitioning, but it will still be a valuable tool to compare the anthropogenic contribution to the ABSOA in the mixed systems. The model estimate could be compared to experimental results in two cases. The method overestimates the ASOA in the 11/6 (toluene) and the 14/6 (xylene) experiments by 40 % respectively 50 %. We therefore divided the contributions calculated by the model by a factor of 1.4.

ACPD
12, 20311–20350, 2012

4 Result and discussion

4.1 Anthropogenic SOA yields

Figure 2 provides the derived ASOA yields as a function of organic aerosol mass (C_{OA}) for the 17 experiments listed in Table 1. The yields are increasing with the organic aerosol load C_{OA} as expected from Raoul's law (Pankow, 1994). A Hill function was fitted to the yields from all anthropogenic experiments resulting in the following expression

$$\text{yield} = \frac{0.39}{1 + \left(\frac{29.7}{C_{OA}}\right)^{0.79}} \quad (2)$$

The parameter base $= 7.4 \times 10^{-4}$ (yield for $C_{OA} \rightarrow 0$ in the Hill function) was set to 0 and the value of 0.39 in the enumerator predicts the maximum yield at infinite C_{OA} to be expected from the aromatic compounds.

The data are within the errors in agreement with previous studies using artificial sunlight for OH production (Hildebrandt et al., 2009), however at the low end site. Hildebrandt et al. (2009) corrected their yields for vapour deposition to the chamber walls or to particles deposited at the walls. The difference could thus be due to neglection of such wall effects in our case. Assuming the corrections applied by Hildebrandt et al. were correct the results indicate that wall effects in SAPHIR affect SOA yields to less than 33 %. For the model calculations of the anthropogenic contributions in the mixed experiments we adopted the Hill function with the parameters derived above, as it phenomenologically will present our observation better than the Hildebrandt results (Hildebrandt et al., 2009, 2011). The principle statements derived are not affected by this choice.

ACPD
12, 20311–20350, 2012

4.2 Mixed anthropogenic/biogenic secondary organic aerosols (ABSOA)

Figure 3 shows the experiment ABSOA 22/6. Ozonolysis and reaction with OH radicals quickly convert the biogenic precursors α-pinene and limonene while toluene is more slowly removed by OH producing a mixed aerosol (upper panel a in Fig. 3). The aerosol is in the beginning dominated by biogenic SOA with slowly increasing anthropogenic contributions later during the course of the photo-oxidation part of the experiment (total OH dose 5×10^{10} cm^{-3} s). The model estimated biogenic and anthropogenic contributions are shown as green and blue dashed lines (Fig. 3a). At the end of the experiment filter samples were collected and analysed for specific acids. In Fig. 3a (inset) results are shown from the filter analysis for a number of identified carboxylic acids and dimer esters. In the lower panel B of Fig. 3 are the properties of the aerosol as a function of time are shown, which correspond to concentration evolution shown in the upper panel. The volume fraction remaining that is non-volatile at a given temperature (exemplified by VFR_{343K}, VFR_{373K}, VFR_{423K}, and VFR_{463K}), f44 and O/C are increasing with time and OH dose, while f43, which is a measure of the less oxidized compound, is decreasing. The f44 is closely related to O/C but the f44 is generally of higher quality (less noise) due to the higher sensitivity of the AMS measurements in the *V* mode and consequently f44 is replacing O/C in parts of the evaluation. The behaviour of VFR was similar at all temperatures and VFR_{343K} will be used as an example in the following discussions. VFR continues to increase at all temperatures in the dark after the roof chamber is closed. This phenomenon was also observed in the other experiments, and indicates that non-photochemical processes must take place. Since O/C, f44, and f43 are levelling off when the roof is closed (duration >6 h), the processes may be even non-oxidative.

Generally, the time behaviour of f44, f43, O/C and volatility are in accordance with previous studies on SOA ageing (Tritscher et al., 2011; Salo et al., 2011). The complication in our experiments is that in addition to OH induced ageing and dark ageing of the SOA also the relative contribution of ASOA and BSOA is changing with time as

ACPD
12, 20311–20350, 2012

can be seen in the ASOA fraction (blue line in Fig. 3b) with the final ASOA fraction estimated to about 56 %.

Table 2 provides the average of selected quantities at the end of the experiments, i.e. when the filters were taken. For ABSOA 22/6 one can see that the reaction mixture was exposed to a relatively high OH dose (5×10^{10} cm^{-3} s) thus producing a persistent (high VFR_{343K}), aged aerosol with rather high O/C ratio (0.59 ± 0.05) and a significant fraction of anthropogenic SOA (≈ 56 %). For the other ABSOA and BSOA experiments the O/C ratios are lower.

For the pure ASOA 13/11 experiment the O/C ratio is high (0.79). It should be noted that in all ABSOA experiments except the 22/6, the AVOC and BVOC were added successively, which had implication on the final anthropogenic fraction. In Table 2 the OH dose is provided separately for the AVOC and BVOC taking into account when AVOC and BVOC, respectively, were added into the chamber. If for example comparing the ABSOA 11-12/6 with ABSOA 14-15/6 the BVOC are exposed to more OH in experiment 14-15/6 providing increased VFR_{343K} at somewhat higher O/C ratio. Note that in exp. 11-12/6 the mixing fan broke during the first day. This affects the observed SOA mass as the lifetime of SOA in the SAPHIR chamber is longer with the fan switched off (Salo et al., 2011).

Since the properties of the aerosol at the time of filter sampling and the end of the experiment depend on several aspects such as OH dose, reaction time and sequence of addition a more thorough analysis was necessary as described below. However, generally from the values provided in Table 2 one may conclude that increasing anthropogenic fraction and OH dose provided an aerosol with higher O/C ratio and VFR_{343K} thus higher persistency.

4.3 Speciation and compound classes in filter measurements

Figure 4 shows total ion chromatograms of organic acids from the filter samples for two experiments, ASOA 11/6 and ABSOA 12/6. Exp. 11/6 shows fewer organic acids in ASOA from toluene compared to the number of organic acids in ABSOA, though it

ACPD
12, 20311–20350, 2012

is important to note that the analytical method will primarily detect organic acids and not less polar molecules such as carbonyl compounds that could also contribute to SOA. The respective chromatogram of exp. 10/6 resembles that of exp. 11/6. SOA from photo-oxidation of toluene at high NO_x conditions have been observed to consist of a high number of carbonyl compounds as well as small organic acids (Kleindienst et al., 2004), which may be difficult to detect using the applied analytical conditions.

Table 3 lists selected identified and quantified oxidation products of the precursors α-pinene and limonene. Quantification of identified α-pinene products showed strikingly similar concentrations (relative to total aerosol mass) within 15 % in aerosol samples from experiments 10/6 and 12/6. This proves that there is a very good reproducibility of both the SAPHIR chamber experiments and chemical analysis. Exp. 10/6 and 12/6 primarily differ in the order of introduction of VOC reactants to the SAPHIR chamber, where BVOC mix was added before toluene in exp. 10/6, while toluene was aged for 5.75 h before addition of BVOC mix in exp. 12/6. Since the concentrations of oxidation products from α-pinene are quite similar in the two experiments, this indicates that the presence of toluene ASOA in the chamber prior to BVOC introduction does not significantly affect the composition of BSOA tracers for α-pinene given in Table 3.

The α-pinene oxidation products can be grouped in first-generation products (a broadly defined group consisting of pinonic acid, *cis*-pinic acid, terpenylic acid and diaterpenylic acid acetate), an identified second-generation product MBTCA previously identified from gas-phase OH oxidation of pinonic acid (Müller et al., 2012) and suggested as tracer for pinene oxidation (Szmigielski et al., 2007) and dimer esters of α-pinene oxidation products. The group of dimer esters covers the following specifically identified compounds: pinyl-diaterpenyl dimer ester (molecular weight, MW 358), pinonyl-pinyl dimer ester (MW 368) and terpenyl-diaterpenyl dimer ester (MW 344) previously observed from ozonolysis of α-pinene and β-pinene (Müller et al., 2008, 2009; Camredon et al., 2010; Yasmeen et al., 2010; Gao et al., 2010; Kristensen et al., 2012). The class concentration of the particulate organic matter are shown in Table 3 and presented in Fig. 5. In experiments 10/6 and 12/6, first generation α-pinene oxidation

ACPD
12, 20311–20350, 2012

products contribute about 3 % to the aerosol mass, while the second generation product contributes only about 0.03 %. Dimer esters constitute about twice as much of the aerosol in exp. 10/6 compared to exp. 12/6 (0.09 % and 0.04 % of the aerosol mass, respectively), which is probably due to the order of magnitude higher OH dose in exp. 10/6. In exp. 14–15/6 which differs from exp. 11/6–12/6 in the use of xylene instead of toluene, only 40 % of the aerosol mass was left when the filters were taken. The higher value in exp. 11–12/6 could be traced back to prolonged the SOA lifetime in the chamber.

In exp. 22/6 BVOC mix and toluene were added together to the SAPHIR chamber at the same time and the concentration of BVOC was about one fourth of the previous experiments. This is reflected in the total aerosol mass at the end of the experiment which was 3.5 $\mu g\,m^{-3}$, about one fourth of exp. 10/6 and 12/6 (16.5 and 14.6 $\mu g\,m^{-3}$, respectively). The lower BVOC concentration used in exp. 22/6 results in a generally lower concentration of almost all identified compounds compared to exp. 10/6 and 12/6 (Table 3). Interestingly, the second-generation oxidation product MBTCA however shows a significantly higher concentration in exp. 22/6 compared to exp. 10/6 and 12/6 constituting almost 1.4 % of the total aerosol mass (Fig. 5). A possible explanation for the higher concentration of MBTCA in exp. 22/6 could be the higher OH-to-BVOC ratio compared to exp. 10/6 and 12/6 which could increase the gas-phase oxidation and ageing of first-generation oxidation products such as *cis*-pinonic acid. Increased ageing in exp. 22/6 may also explain the relatively high fraction of dimer esters (0.33 % of the aerosol mass) compared to exp. 10/6 and 12/6. This exp. 22/6 with the highest MBTCA fraction features also the largest O/C and VFR_{343K} of all ABSOA experiments (Table 2).

4.4 Persistency (VFR) as function of time, OH dosis and degree of oxidation

Figure 6 illustrates VFR_{343K} of five experiments where AVOC is represented by toluene or xylene, and BVOC is represented by equal amounts of α-pinene and limonene. To entangle the effects of photochemistry, processes in the dark and anthropogenic

ACPD
12, 20311–20350, 2012

contribution, VFR_{343K} is displayed as function of experiment duration (upper panel), OH dose (middle panel) and f44 (lower panel). In all panels the size of the markers corresponds to the model-estimated anthropogenic fraction of SOA.

In Fig. 6a the time evolution of VFR_{343K} is shown as a function of elapsed time, where the starting time was defined by the start of particle formation induced either by opening the roof or by injection of AVOC into the illuminated chamber. The corresponding points in time of the VFR_{343K} measurements are indicated in Fig. 1. During the first 6 or 9 h, respectively, when the reaction mixtures are exposed to sun light, the SOA become less volatile reflected as an increase of VFR_{343K}, no matter whether ASOA, ABSOA or BSOA was available. Figure 6a illustrate also that VFR_{343K} may increases with increasing anthropogenic contribution, with pure BSOA (10/6, first data point) at the bottom and pure ASOA 11/6, 13/6 and 14/6 grouping at the top of the VFR_{343K} scale. The ABSOA experiment 22/6 wherein AVOC and BVOC were mixed from the beginning is situated in between the pure systems.

In the two cases 11/6 and 14/6 when BVOC were added in the dark to pre-existing ASOA a significant drop in VFR_{343K} is observed. The drop is due to condensation of fresh BSOA material arising from the ozonolysis of the BVOC. (Ozone was available from the previous photochemical processes.) The fresh BSOA component is leading to a much more volatile aerosol. However, the formed ABSOA is then getting less volatile during the night reflected as an increase of the VFR_{343K}. In both cases the roof was opened the second day after about 23 h. In the experiment 15/6 the photo-oxidation of BVOC and xylene formed fresh particulate material again generating more volatile aerosol. This is consistent with previous results (Salo et al., 2011) emphasising the importance of gas phase chemistry in the OH radical induced ageing of SOA. At the end of 15/6 the VFR_{343K} recovered and exceeds the value before light exposure, indicating that the ageing process continued after the production of fresh material had ceased, forming a more persistent SOA. The corresponding dip in VFR_{343K} was not seen in the toluene case 12/6 as the extra photo-oxidation did only add a small increase in SOA mass. The OH dose acting at the second day of experiment 15/6 is about

ACPD
12, 20311–20350, 2012

twice that of the exp. 12/6 (see below Fig. 6B) in accordance with production of more fresh material on 15/6. It is noted that the filter analysis revealed more 2nd generation product at the end of exp. 15/6 in accordance with the higher VFR_{343K} on this day.

Figure 6b displays the VFR_{343K} as a function of the actual OH dose derived from the OH-LIF measurements. The lowest dose on the scale corresponds to 1.5 h exposure to average atmospheric OH levels of 2×10^6 cm^{-3}, whereas the largest dose corresponds to 12 h exposure. For the aerosols in the dark, any change in the VFR_{343K} falls on vertical lines at that OH dose seen by the pre-existing SOA. This OH dose has to be subtracted in order to get the actual OH dose acting on the added BSOA components during the photo-chemical ageing on the next day.

Presenting VFR_{343K} vs. the OH dose simplifies the picture for the first hours. Overall, the VFR of SOA increases with OH dose and the higher VFR_{343K} for ASOA is partly caused by exposure to a larger OH dose. Experiment 15/6 and 22/6 show higher VFR_{343K} compared to exp. 10/6 and 12/6, which were exposed to smaller OH dose. The latter have both lower 2nd generation product fraction compared to 15/6 and 22/6, and smaller dimer fractions than exp. 22/6 (Fig. 5). We conclude that the ageing and formation of a less volatile aerosol, reflected as an increase of VFR, is overall related to the OH dose, thus to photo-chemistry. The influence of the photo-chemistry on the BSOA components is also reflected in increasing 2nd generation product and to less extent the dimer fraction.

For the pure ASOA the relative increase of VFR_{343K} with OH dose is less pronounced, compared to ABSOA and BSOA dominated aerosols. The onset of ASOA particle formation and the first available VFR_{343K} data occur at larger OH dose, due to the lower reactivity of the AVOC. In addition first generation oxidation products of AVOC (mainly carbonyls see above) may have higher vapour pressures compared to the BVOC and more oxidation steps are needed to induce SOA formation. As a consequence the potential of ageing after particle formation is smaller for ASOA, since the vapours aged already in the gas-phase prior to particle formation. In contrast BSOA from the reactive precursors α-pinene and limonene is formed already at low OH dose.

ACPD
12, 20311–20350, 2012

In addition, during rapid formation, vapours with higher vapour pressures also reach saturation and contribute to the BSOA mass (Pankow, 1994; Odum et al., 1996), leading to a higher volatility early in the formation phase. These vapours will react (age) with OH and this leads to increasing low volatile second generation products e.g. MBTCA (Müller et al., 2012). The curve for the mixed ABSOA (22/6) is connecting the BSOA experiment with the ASOA regime, as significant ASOA fraction is building up during the formation process (comp. Fig. 3a). Interestingly, for the exp. 10/6 where toluene was added to pre-existing BSOA, the VFR_{343K} increase of the ABSOA with OH dose accelerates with increasing ASOA contribution. This behaviour is distinct although only up to 8–9 % of the aerosol is calculated to be ASOA (Table 3). This suggests that even small contributions of ASOA can reduce the volatility and enhance the persistence of ABSOA.

After the roof was closed at the end of the day we took one data point in the dark with all other parameters unchanged. The VFR_{343K} continues to increase consistently for all investigated ASOA and ABSOA systems. One toluene experiment (13/6) was exposed to more OH than the others but still showed indications for ageing under dark conditions, however weaker. Since the volatility of ABSOA decreases also in the dark, the enhancement during daytime in experiment (10/6) may also have non-oxidative contributions. Night time ageing processes were reported before by Tritscher et al. (2011) for α-pinene SOA.

Figure 6c shows the VFR_{343K} as function of f44, which is related to the O/C ratio for biogenic and aromatic systems (Aiken et al., 2008; Chhabra et al., 2010, 2011). Simplistically, a higher f44 indicates increasing contribution of carboxylic acids. Here we deploy less data points since the detection level was insufficient for the xylene ASOA.

The two pure ASOA systems show high VFR_{343K}, and the largest f44 signal at 0.2 and $\sim$ 0.25, respectively. The f44 are larger than f44 reported by Chhabra et al. (2011) (0.05–0.1) and in the range of f44 reported by Aiken et al. (2008) for ambient urban aerosol. For the ASOA in exp. 11/6 the standard deviation of f44 is large (0.09) while in

ACPD
12, 20311–20350, 2012

exp. 13/6 it is significantly lower (0.004). A difference between these two experiments is that in the 13/6 a small addition of NO_x was made but from the yield curve shown in Fig. 2 this should not influence the aerosol production. Considering the large scatter of the f44 data on the 11/6 we neglect this data for the further considerations and assume that pure ASOA systems have f44 of 0.2 in line with the 13/6 experiments. Independent of that, the large observed f44 for pure ASOA corroborates our suggestion that more oxidation steps are needed and that AVOC vapours are more oxidized before they form particulate matter, probably because they have smaller C-backbones.

The fresh mixed ABSOA 22/6 features low VFR_{343K} of 0.79 at f44 of 0.11. During on-going photo-oxidation VFR_{343K} is increasing with increasing f44. At f44 of 0.15 the VFR_{343K} of the ABSOA reaches values in between the pure BSOA with f44 $\approx$ 0.1 and the pure ASOA systems with f44org $\sim$ 0.2. This observation corroborates our model estimate of $\approx$ 60 % anthropogenic contribution, as – assuming linear mixing behaviour – a f44 = 0.15 indicates a 50/50 mixture of BSOA and ASOA, when pure BSOA has a f44 of 0.1. An increase of f44 is also seen in exp. 10/6 after toluene was added to the BSOA aerosol. The increase of VFR_{343K} with f44 in experiment 10/6 is similar to 22/6, but shifted to 20 % lower f44 values. The large change in VFR_{343K} with f44 for both ABSOA experiments supports that the presence of ASOA components enhances the persistence of the aerosols, possibly in a non-stoichiometric fashion. The strong tendency to increase VFR with only small changes in oxidation state would be commensurable with oligomerisation processes, which were first described for trimethylbenzene, also an aromatic precursor (Kalberer et al., 2004).

The addition of BVOC to ASOA followed by ozonolysis in exp. 11/6 and 14/6 reduces f44 from about 0.2 to about 0.1 in both cases, i.e. the aerosol is obviously dominated by BSOA. In the ABSOA exp. 12/6 not much change occurred when exposing the ABSOA to sunlight the second day while in the ABSOA 15/6 chemical changes during the dip in VFR_{343K} were observed with f44 increasing with sun exposure and OH dose from 0.10 to 0.11.

ACPD
12, 20311–20350, 2012

In summary, ASOA shows larger VFR_{343K}, i.e. lower volatility associated to higher degree of oxidation than BSOA and ABSOA. To reach the larger degree of oxidation longer exposure to OH radicals is needed. In ABSOA already small fractions of ASOA lead to strong increase in VFR_{343K}, even at low degrees of oxidation, indicating that ASOA components trigger an extra persistence either by oligomerisation or morphological changes e.g. formation of glassy states (Zobrist et al., 2008; Virtanen et al., 2010). Since VFR_{343K} increase also overnight in presence of low ozone concentrations, a slow non-photochemical, if not non-oxidative ageing process must also take place. This process is not much affecting the oxidation state and could be oligomerization by condensation reactions.

5 Atmospheric implications

Oxidation of aromatics and other traditional anthropogenic VOCs can contribute significantly to SOA formation. Using newly derived aerosol yields de Gouw et al. (2008) accounted for a large fraction (37 %) by oxidation of traditional anthropogenic SOA precursors and the remaining fraction remained unexplained. A large unexplained fraction was typical for model and measurements comparisons and has been addressed in several previous studies where e.g. Volkamer et al. (2006) specifically demonstrated how ASOA was under-predicted in urban air masses by up to a factor of 10. During recent years several explanations have been suggested for these inconsistencies. One finding is that SOA formation from aromatic systems has significant higher yields than previously reported which was further recognised in our study (Table 1 and Fig. 2). However, in the study of de Gouw et al. (2008) the higher yields from aromatic system were already applied and 63 % SOA mass was still found unexplained. Other explanations for this gap can be missing primary precursors, oxidation of intermediate volatile compounds and effective ageing of SOA (Pye and Seinfeld, 2010). All these issues have been addressed in a series of modelling studies of air pollution in Mexico as part of the MILAGRO experiment (see e.g. Tsimpidi et al., 2011; Dzepina et al., 2009,

ACPD
12, 20311–20350, 2012

2011; Hodzic et al., 2010). The finding from the present study that mixed ASOA and BSOA can evolve rapidly producing a persistent aerosol with low volatility favours an ageing treatment in models with reduced evaporation upon dilution with increasing OH exposure (Dzepina et al., 2011).

Using a combination of global modelling efforts and observations of OA (AMS) and OC (filters) Spracklen et al. (2011) proposed a new source attribution of SOA. According to their analysis 2/3 of the SOA may have biogenic precursors but is strongly related with the CO source distribution, an anthropogenic tracer. Such effects were proposed before by de Gouw et al. (2005, 2008) and de Gouw and Jimenez (2009). This portion of SOA is called anthropogenic enhanced SOA. Our findings may contribute to understand anthropogenic enhancement. Aromatic emissions are surely closely related to CO emissions and if an ASOA fraction of 10 % or more is available this should increase the persistence of the resulting ABSOA. The persistency enhancement is not available in remote, biogenically dominated regions, where aromatic emissions are absent. Since ABSOA is more persistent than BSOA, less BSOA is observed than ABSOA at same source strength of BVOC. However we also showed that OH dose is an important driver of ageing and persistence of SOA, thus we do not claim that we can fully explain the anthropogenic enhancement. However such effects of aromatics could contribute significantly to anthropogenic enhancement.

The exposure of the reaction mixtures to natural OH dose and the long duration of experiments lead to concentrations of monoterpene oxidation products as listed in Table 3 that are generally higher, but still comparable to concentrations found in aerosol samples from ambient air (Kristensen and Glasius, 2011; Zhang et al., 2010). Dimer esters have previously been identified from ozonolysis of α-pinene in smog chamber studies and ambient air (e.g. Camredon et al., 2010; Kristensen et al., 2012). Our results can be connected to atmospheric conditions using the OH dose, for example the OH dose in BSOA 22/6 is 5.0 X $\times 10^{10}$ cm^{-3} s and corresponds to 7 h of exposure to an OH radical concentration of 2×10^{6} cm^{-3}. The final aerosol mass of 3.6 µg cm^{-3} is also comparable to atmospheric observations of organic aerosol mass in urban plumes

ACPD
12, 20311–20350, 2012

(Tsimpidi et al., 2011). We thus conclude that our findings are transferable to the atmosphere.

6 Conclusions

The main focus of this work was to study aerosol formation and properties from photooxidation of mixed anthropogenic and biogenic precursor to mimic real world conditions. In a separate set of experiments also the aerosol yields of anthropogenic SOA were quantified. The anthropogenic yield data were used to estimate the ASOA contribution to aerosol mass in the mixed ABSOA experiments applying a simplified model. The estimated ASOA contributions ranged from very small (> 1 %) up to significant fraction (> 50 %), providing a suitable range to study the effect of ASOA on aerosol properties. Absolute measurements of OH radicals were used to constrain the estimated conversion of anthropogenic precursor in the mixed experiments and providing a direct measure on OH dose.

The volatility of the aerosol is an important measure of the thermal persistence of particles in the atmosphere, and was used in combination with the OH dose, anthropogenic fraction and chemical composition of the particles to understand the underlying aerosol processes. Aromatic anthropogenic systems produced aerosol with lower volatility than the biogenic system. However, in order to produce significant anthropogenic aerosol fraction the systems were exposed to large OH doses, corresponding to oxidation over several hours at mid-European photochemical conditions. The larger OH dose did also influence the chemical composition as evidenced by higher concentrations of dimer esters and second generation products in the particles. The VFR_{343K} generally increased with increasing OH dose, but if a reactive VOC was added or a system with remaining gas phase vapour was exposed again to sunlight the VFR_{343K} dropped temporarily in analogy to the observation described in Salo et al. (2011). Since the ASOA had a lower volatility than BSOA any changes in the anthropogenic fraction did influence the overall volatility.

ACPD
12, 20311–20350, 2012

In addition to OH induced ageing and the anthropogenic fraction of the particles, the VFR_{343K} was also affected by a time dependent ageing, that occurred during dark hours, and might be linked to condensed phase processes such as polymerisation. The observed volatility changes and associated processes were compared to the chemical composition of the aerosol, O/C and f44 (fraction of $m/z = 44$). Analogous to the VFR_{343K} changes, the O/C ratio increased due to OH induced ageing and with increasing anthropogenic fraction. However, for the third process, that dominated VFR_{343K} changes during dark hours, no relation to O/C ratio could be established. The interpretation is that this process does not change the overall chemical composition but the volatility, and was consequently attributed to changes in viscosity, e.g. induced by polymerisation.

Given the observation in the particulate phase and the exposure to natural sun-light at realistic OH concentrations our findings should be applicable to the atmosphere. The persistence induced by ASOA (and OH dose) have an influence on the atmospheric SOA lifetime, where the BSOA fraction in mixed ABSOA should have longer lifetimes and thus higher abundance in anthropogenically influenced areas with distinct aromatic emissions compared to BSOA in natural regions. This effect should be considered in regional and global model predictions.

Acknowledgements. This project was supported by EUROCHAMP-2 (Integration of European Simulation Chambers for Investigating Atmospheric Processes) – EC 7th framework, Swedish Formas (214-2010-1756), the Swedish Research Council (80 475 101) and the Tellus research platform at University of Gothenburg. The research presented is a contribution to the Swedish strategic research area ModElling the Regional and Global Earth system, MERGE. Sascha Nehr thanks the Deutsche Forschungsgemeinschaft for support under grant BO 1580/3-1. We cordially thank Leah Hildebrandt for providing us her data for comparisons.

The service charges for this open access publication have been covered by a Research Centre of the Helmholtz Association.

ACPD

12, 20311–20350, 2012

References

Aiken, A. C., DeCarlo, P. F., and Jimenez, J. L.: Elemental analysis of organic species with electron ionization high-resolution mass spectrometry, Anal. Chem., 79, 8350–8358, doi:10.1021/ac071150w, 2007.

Aiken, A. C., DeCarlo, P. F., Kroll, J. H., Worsnop, D. R., Huffman, J. A., Docherty, K. S., Ulbrich, I. M., Mohr, C., Kimmel, J. R., Sueper, D., Sun, Y., Zhang, Q., Trimborn, A., Northway, M., Ziemann, P. J., Canagaratna, M. R., Onasch, T. B., Alfarra, M. R., Prevot, A. S. H., Dommen, J., Duplissy, J., Metzger, A., Baltensperger, U., and Jimenez, J. L.: O/C and OM/OC ratios of primary, secondary, and ambient organic aerosols with high-resolution time-of-flight aerosol mass spectrometry, Environ. Sci. Technol., 42, 4478–4485, doi:10.1021/es703009q, 2008.

Aiken, A. C., Salcedo, D., Cubison, M. J., Huffman, J. A., DeCarlo, P. F., Ulbrich, I. M., Docherty, K. S., Sueper, D., Kimmel, J. R., Worsnop, D. R., Trimborn, A., Northway, M., Stone, E. A., Schauer, J. J., Volkamer, R. M., Fortner, E., de Foy, B., Wang, J., Laskin, A., Shutthanandan, V., Zheng, J., Zhang, R., Gaffney, J., Marley, N. A., Paredes-Miranda, G., Arnott, W. P., Molina, L. T., Sosa, G., and Jimenez, J. L.: Mexico City aerosol analysis during MILAGRO using high resolution aerosol mass spectrometry at the urban supersite (T0) – Part 1: Fine particle composition and organic source apportionment, Atmos. Chem. Phys., 9, 6633–6653, doi:10.5194/acp-9-6633-2009, 2009.

Allan, J. D., Delia, A. E., Coe, H., Bower, K. N., Alfarra, M. R., Jimenez, J. L., Middlebrook, A. M., Drewnick, F., Onasch, T. B., Canagaratna, M. R., Jayne, J. T., and Worsnop, D. R.: A generalised method for the extraction of chemically resolved mass spectra from aerodyne aerosol mass spectrometer data, J. Aerosol Sci., 35, 909–922, doi:10.1016/j.jaerosci.2004.02.007, 2004.

Berndt, T. and Boge, O.: Rate constants for the gas-phase reaction of hexamethylbenzene with OH radicals and H atoms and of 1,3,5-trimethylbenzene with H atoms, Int. J. Chem. Kinet., 33, 124–129, doi:10.1002/1097-4601(200102)33:2<124::aid-kin1004>3.0.co;2-s, 2001.

Bohn, B., Rohrer, F., Brauers, T., and Wahner, A.: Actinometric measurements of NO_2 photolysis frequencies in the atmosphere simulation chamber SAPHIR, Atmos. Chem. Phys., 5, 493–503, doi:10.5194/acp-5-493-2005, 2005.

Camredon, M., Hamilton, J. F., Alam, M. S., Wyche, K. P., Carr, T., White, I. R., Monks, P. S., Rickard, A. R., and Bloss, W. J.: Distribution of gaseous and particulate organic composition

ACPD
12, 20311–20350, 2012

during dark α-pinene ozonolysis, Atmos. Chem. Phys., 10, 2893–2917, doi:10.5194/acp-10-2893-2010, 2010.
Carlton, A. G., Pinder, R. W., Bhave, P. V., and Pouliot, G. A.: To what extent can biogenic SOA be controlled?, Environ. Sci. Technol., 44, 3376–3380, doi:10.1021/es903506b, 2010.
Chhabra, P. S., Flagan, R. C., and Seinfeld, J. H.: Elemental analysis of chamber organic aerosol using an aerodyne high-resolution aerosol mass spectrometer, Atmos. Chem. Phys., 10, 4111–4131, doi:10.5194/acp-10-4111-2010, 2010.
Chhabra, P. S., Ng, N. L., Canagaratna, M. R., Corrigan, A. L., Russell, L. M., Worsnop, D. R., Flagan, R. C., and Seinfeld, J. H.: Elemental composition and oxidation of chamber organic aerosol, Atmos. Chem. Phys., 11, 8827–8845, doi:10.5194/acp-11-8827-2011, 2011.
de Gouw, J. A. and Jimenez, J. L.: Organic aerosols in the Earth's atmosphere, Environ. Sci. Technol., 43, 7614–7618, doi:10.1021/es9006004, 2009.
de Gouw, J. A., Middlebrook, A. M., Warneke, C., Goldan, P. D., Kuster, W. C., Roberts, J. M., Fehsenfeld, F. C., Worsnop, D. R., Canagaratna, M. R., Pszenny, A. A. P., Keene, W. C., Marchewka, M., Bertman, S. B., and Bates, T. S.: Budget of organic carbon in a polluted atmosphere: results from the New England Air Quality Study in 2002, J. Geophys. Res.-Atmos., 110, D16305, doi:10.1029/2004jd005623, 2005.
de Gouw, J. A., Brock, C. A., Atlas, E. L., Bates, T. S., Fehsenfeld, F. C., Goldan, P. D., Holloway, J. S., Kuster, W. C., Lerner, B. M., Matthew, B. M., Middlebrook, A. M., Onasch, T. B., Peltier, R. E., Quinn, P. K., Senff, C. J., Stohl, A., Sullivan, A. P., Trainer, M., Warneke, C., Weber, R. J., and Williams, E. J.: Sources of particulate matter in the Northeastern United States in summer: 1. Direct emissions and secondary formation of organic matter in urban plumes, J. Geophys. Res.-Atmos., 113, D08301, doi:10.1029/2007jd009243, 2008.
DeCarlo, P. F., Kimmel, J. R., Trimborn, A., Northway, M. J., Jayne, J. T., Aiken, A. C., Gonin, M., Fuhrer, K., Horvath, T., Docherty, K. S., Worsnop, D. R., and Jimenez, J. L.: Field-deployable, high-resolution, time-of-flight aerosol mass spectrometer, Anal. Chem., 78, 8281–8289, doi:10.1021/ac061249n, 2006.
Derwent, R. G., Jenkin, M. E., Utembe, S. R., Shallcross, D. E., Murrells, T. P., and Passant, N. R.: Secondary organic aerosol formation from a large number of reactive man-made organic compounds, Sci. Total Environ., 408, 3374–3381, doi:10.1016/j.scitotenv.2010.04.013, 2010.
Dzepina, K., Volkamer, R. M., Madronich, S., Tulet, P., Ulbrich, I. M., Zhang, Q., Cappa, C. D., Ziemann, P. J., and Jimenez, J. L.: Evaluation of recently-proposed secondary organic

ACPD
12, 20311–20350, 2012

aerosol models for a case study in Mexico City, Atmos. Chem. Phys., 9, 5681–5709, doi:10.5194/acp-9-5681-2009, 2009.
Dzepina, K., Cappa, C. D., Volkamer, R. M., Madronich, S., DeCarlo, P. F., Zaveri, R. A., and Jimenez, J. L.: Modeling the multiday evolution and aging of secondary organic aerosol during MILAGRO 2006, Environ. Sci. Technol., 45, 3496–3503, doi:10.1021/es103186f, 2011.
Fuchs, H., Dorn, H.-P., Bachner, M., Bohn, B., Brauers, T., Gomm, S., Hofzumahaus, A., Holland, F., Nehr, S., Rohrer, F., Tillmann, R., and Wahner, A.: Comparison of OH concentration measurements by DOAS and LIF during SAPHIR chamber experiments at high OH reactivity and low NO concentration, Atmos. Meas. Tech. Discuss., 5, 2077–2110, doi:10.5194/amtd-5-2077-2012, 2012.
Fushimi, A., Wagai, R., Uchida, M., Hasegawa, S., Takahashi, K., Kondo, M., Hirabayashi, M., Morino, Y., Shibata, Y., Ohara, T., Kobayashi, S., and Tanabe, K.: Radiocarbon ((14)C) diurnal variations in fine particles at sites downwind from Tokyo, Japan in Summer, Environ. Sci. Technol., 45, 6784–6792, doi:10.1021/es201400p, 2011.
Galloway, M. M., Loza, C. L., Chhabra, P. S., Chan, A. W. H., Yee, L. D., Seinfeld, J. H., and Keutsch, F. N.: Analysis of photochemical and dark glyoxal uptake: implications for SOA formation, Geophys. Res. Lett., 38, L17811, doi:10.1029/2011gl048514, 2011.
Gao, Y. Q., Hall, W. A., and Johnston, M. V.: Molecular composition of monoterpene secondary organic aerosol at low mass loading, Environ. Sci. Technol., 44, 7897–7902, doi:10.1021/es101861k, 2010.
Glasius, M., la Cour, A., and Lohse, C.: Fossil and nonfossil carbon in fine particulate matter: a study of five European cities, J. Geophys. Res.-Atmos., 116, D11302, doi:10.1029/2011jd015646, 2011.
Goldstein, A. H. and Galbally, I. E.: Known and unexplored organic constituents in the Earth's atmosphere, Environ. Sci. Technol., 41, 1514–1521, 2007.
Hallquist, M., Wenger, J. C., Baltensperger, U., Rudich, Y., Simpson, D., Claeys, M., Dommen, J., Donahue, N. M., George, C., Goldstein, A. H., Hamilton, J. F., Herrmann, H., Hoffmann, T., Iinuma, Y., Jang, M., Jenkin, M. E., Jimenez, J. L., Kiendler-Scharr, A., Maenhaut, W., McFiggans, G., Mentel, Th. F., Monod, A., Prévôt, A. S. H., Seinfeld, J. H., Surratt, J. D., Szmigielski, R., and Wildt, J.: The formation, properties and impact of secondary organic aerosol: current and emerging issues, Atmos. Chem. Phys., 9, 5155–5236, doi:10.5194/acp-9-5155-2009, 2009.

ACPD
12, 20311–20350, 2012

Heald, C. L., Kroll, J. H., Jimenez, J. L., Docherty, K. S., DeCarlo, P. F., Aiken, A. C., Chen, Q., Martin, S. T., Farmer, D. K., and Artaxo, P.: A simplified description of the evolution of organic aerosol composition in the atmosphere, Geophys. Res. Lett., 37, L08803, doi:10.1029/2010gl042737, 2010.

Hildebrandt, L., Donahue, N. M., and Pandis, S. N.: High formation of secondary organic aerosol from the photo-oxidation of toluene, Atmos. Chem. Phys., 9, 2973–2986, doi:10.5194/acp-9-2973-2009, 2009.

Hildebrandt, L., Henry, K. M., Kroll, J. H., Worsnop, D. R., Pandis, S. N., and Donahue, N. M.: Evaluating the mixing of organic aerosol components using high-resolution aerosol mass spectrometry, Environ. Sci. Technol., 45, 6329–6335, doi:10.1021/es200825g, 2011.

Hodzic, A., Jimenez, J. L., Madronich, S., Canagaratna, M. R., DeCarlo, P. F., Kleinman, L., and Fast, J.: Modeling organic aerosols in a megacity: potential contribution of semi-volatile and intermediate volatility primary organic compounds to secondary organic aerosol formation, Atmos. Chem. Phys., 10, 5491–5514, doi:10.5194/acp-10-5491-2010, 2010.

Hoyle, C. R., Boy, M., Donahue, N. M., Fry, J. L., Glasius, M., Guenther, A., Hallar, A. G., Huff Hartz, K., Petters, M. D., Petäjä, T., Rosenoern, T., and Sullivan, A. P.: A review of the anthropogenic influence on biogenic secondary organic aerosol, Atmos. Chem. Phys., 11, 321–343, doi:10.5194/acp-11-321-2011, 2011.

Hu, D., Bian, Q., Li, T. W. Y., Lau, A. K. H., and Yu, J. Z.: Contributions of isoprene, monoterpenes, beta-caryophyllene, and toluene to secondary organic aerosols in Hong Kong during the summer of 2006, J. Geophys. Res.-Atmos., 113, D22206, doi:10.1029/2008jd010437, 2008.

Jaoui, M., Edney, E. O., Kleindienst, T. E., Lewandowski, M., Offenberg, J. H., Surratt, J. D., and Seinfeld, J. H.: Formation of secondary organic aerosol from irradiated alpha-pinene/toluene/NO(x) mixtures and the effect of isoprene and sulfur dioxide, J. Geophys. Res.-Atmos., 113, D09303, doi:10.1029/2007jd009426, 2008.

Jimenez, J. L., Canagaratna, M. R., Donahue, N. M., Prevot, A. S. H., Zhang, Q., Kroll, J. H., DeCarlo, P. F., Allan, J. D., Coe, H., Ng, N. L., Aiken, A. C., Docherty, K. S., Ulbrich, I. M., Grieshop, A. P., Robinson, A. L., Duplissy, J., Smith, J. D., Wilson, K. R., Lanz, V. A., Hueglin, C., Sun, Y. L., Tian, J., Laaksonen, A., Raatikainen, T., Rautiainen, J., Vaattovaara, P., Ehn, M., Kulmala, M., Tomlinson, J. M., Collins, D. R., Cubison, M. J., Dunlea, E. J., Huffman, J. A., Onasch, T. B., Alfarra, M. R., Williams, P. I., Bower, K., Kondo, Y., Schneider, J., Drewnick, F., Borrmann, S., Weimer, S., Demerjian, K., Salcedo, D., Cottrell, L., Grif-

ACPD
12, 20311–20350, 2012

fin, R., Takami, A., Miyoshi, T., Hatakeyama, S., Shimono, A., Sun, J. Y., Zhang, Y. M., Dzepina, K., Kimmel, J. R., Sueper, D., Jayne, J. T., Herndon, S. C., Trimborn, A. M., Williams, L. R., Wood, E. C., Middlebrook, A. M., Kolb, C. E., Baltensperger, U., and Worsnop, D. R.: Evolution of organic aerosols in the atmosphere, Science, 326, 1525–1529, doi:10.1126/science.1180353, 2009.

Jonsson, Å. M., Hallquist, M., and Saathoff, H.: Volatility of secondary organic aerosols from the ozone initiated oxidation of [alpha]-pinene and limonene, J. Aerosol Sci., 38, 843–852, 2007.

Jordan, A., Haidacher, S., Hanel, G., Hartungen, E., Mark, L., Seehauser, H., Schottkowsky, R., Sulzer, P., and Mark, T. D.: A high resolution and high sensitivity proton-transfer-reaction time-of-flight mass spectrometer (PTR-TOF-MS), Int. J. Mass Spectrom., 286, 122–128, doi:10.1016/j.ijms.2009.07.005, 2009.

Kalberer, M., Paulsen, D., Sax, M., Steinbacher, M., Dommen, J., Prevot, A. S. H., Fisseha, R., Weingartner, E., Frankevich, V., Zenobi, R., and Baltensperger, U.: Identification of polymers as major components of atmospheric organic aerosols, Science, 303, 1659–1662, doi:10.1126/science.1092185, 2004.

Kanakidou, M., Seinfeld, J. H., Pandis, S. N., Barnes, I., Dentener, F. J., Facchini, M. C., Van Dingenen, R., Ervens, B., Nenes, A., Nielsen, C. J., Swietlicki, E., Putaud, J. P., Balkanski, Y., Fuzzi, S., Horth, J., Moortgat, G. K., Winterhalter, R., Myhre, C. E. L., Tsigaridis, K., Vignati, E., Stephanou, E. G., and Wilson, J.: Organic aerosol and global climate modelling: a review, Atmos. Chem. Phys., 5, 1053–1123, doi:10.5194/acp-5-1053-2005, 2005.

Kautzman, K. E., Surratt, J. D., Chan, M. N., Chan, A. W. H., Hersey, S. P., Chhabra, P. S., Dalleska, N. F., Wennberg, P. O., Flagan, R. C., and Seinfeld, J. H.: Chemical composition of gas- and aerosol-phase products from the photooxidation of naphthalene, J. Phys. Chem. A, 114, 913–934, doi:10.1021/jp908530s, 2010.

Kleindienst, T. E., Conver, T. S., McIver, C. D., and Edney, E. O.: Determination of secondary organic aerosol products from the photooxidation of toluene and their implications in ambient $PM_{2.5}$, J. Atmos. Chem., 47, 79–100, doi:10.1023/b:joch.0000012305.94498.28, 2004.

Kristensen, K. and Glasius, M.: Organosulfates and oxidation products from biogenic hydrocarbons in fine aerosols from a forest in North West Europe during spring, Atmos. Environ., 45, 4546–4556, doi:10.1016/j.atmosenv.2011.05.063, 2011.

ACPD
12, 20311–20350, 2012

Kristensen, K., Enggrob, K. L., Platt, S., Mortensen, R., Worton, D. R., Surratt, J. D., Bilde, M., Goldstein, A. H., and Glasius, M.: Formation and occurrence of dimers of monoterpene oxidation products in atmospheric aerosols, Atmos. Chem. Phys., submitted, 2012.

Kroll, J. H. and Seinfeld, J. H.: Chemistry of secondary organic aerosol: formation and evolution of low-volatility organics in the atmosphere, Atmos. Environ., 42, 3593–3624, 2008.

Lambe, A. T., Onasch, T. B., Massoli, P., Croasdale, D. R., Wright, J. P., Ahern, A. T., Williams, L. R., Worsnop, D. R., Brune, W. H., and Davidovits, P.: Laboratory studies of the chemical composition and cloud condensation nuclei (CCN) activity of secondary organic aerosol (SOA) and oxidized primary organic aerosol (OPOA), Atmos. Chem. Phys., 11, 8913–8928, doi:10.5194/acp-11-8913-2011, 2011.

Müller, L., Reinnig, M.-C., Warnke, J., and Hoffmann, Th.: Unambiguous identification of esters as oligomers in secondary organic aerosol formed from cyclohexene and cyclohexene/α-pinene ozonolysis, Atmos. Chem. Phys., 8, 1423–1433, doi:10.5194/acp-8-1423-2008, 2008.

Müller, L., Reinnig, M.-C., Hayen, H., and Hoffmann, T.: Characterization of oligomeric compounds in secondary organic aerosol using liquid chromatography coupled to electrospray ionization Fourier transform ion cyclotron resonance mass spectrometry, Rapid Commun. Mass Sp., 23, 971–979, doi:10.1002/rcm.3957, 2009.

Müller, L., Reinnig, M.-C., Naumann, K. H., Saathoff, H., Mentel, T. F., Donahue, N. M., and Hoffmann, T.: Formation of 3-methyl-1,2,3-butanetricarboxylic acid via gas phase oxidation of pinonic acid – a mass spectrometric study of SOA aging, Atmos. Chem. Phys., 12, 1483–1496, doi:10.5194/acp-12-1483-2012, 2012.

Odum, J. R., Hoffmann, T., Bowman, F., Collins, D., Flagan, R. C., and Seinfeld, J. H.: Gas/particle partitioning and secondary organic aerosol yields, Environ. Sci. Technol., 30, 2580–2585, doi:10.1021/es950943+, 1996.

Pankow, J. F.: An absorption model of gas/particle partitioning of organic compounds in the atmosphere, Atmos. Environ., 28, 185–188, 1994.

Pye, H. O. T. and Seinfeld, J. H.: A global perspective on aerosol from low-volatility organic compounds, Atmos. Chem. Phys., 10, 4377–4401, doi:10.5194/acp-10-4377-2010, 2010.

Rohrer, F., Bohn, B., Brauers, T., Brüning, D., Johnen, F.-J., Wahner, A., and Kleffmann, J.: Characterisation of the photolytic HONO-source in the atmosphere simulation chamber SAPHIR, Atmos. Chem. Phys., 5, 2189–2201, doi:10.5194/acp-5-2189-2005, 2005.

ACPD
12, 20311–20350, 2012

Salo, K., Hallquist, M., Jonsson, Å. M., Saathoff, H., Naumann, K.-H., Spindler, C., Tillmann, R., Fuchs, H., Bohn, B., Rubach, F., Mentel, Th. F., Müller, L., Reinnig, M., Hoffmann, T., and Donahue, N. M.: Volatility of secondary organic aerosol during OH radical induced ageing, Atmos. Chem. Phys., 11, 11055–11067, doi:10.5194/acp-11-11055-2011, 2011.

Shantz, N. C., Aklilu, Y. A., Ivanis, N., Leaitch, W. R., Brickell, P. C., Brook, J. R., Cheng, Y., Halpin, D., Li, S. M., Tham, Y. A., Toom-Sauntry, D., Prenni, A. J., and Graham, L.: Chemical and physical observations of particulate matter at Golden Ears Provincial Park from anthropogenic and biogenic sources, Atmos. Environ., 38, 5849–5860, doi:10.1016/j.atmosenv.2004.01.050, 2004.

Spracklen, D. V., Jimenez, J. L., Carslaw, K. S., Worsnop, D. R., Evans, M. J., Mann, G. W., Zhang, Q., Canagaratna, M. R., Allan, J., Coe, H., McFiggans, G., Rap, A., and Forster, P.: Aerosol mass spectrometer constraint on the global secondary organic aerosol budget, Atmos. Chem. Phys., 11, 12109–12136, doi:10.5194/acp-11-12109-2011, 2011.

Steinbrecher, R., Klauer, M., Hauff, K., Stockwell, W. R., Jaeschke, W., Dietrich, T., and Herbert, F.: Biogenic and anthropogenic fluxes of non-methane hydrocarbons over an urban-impacted forest, Frankfurter Stadtwald, Germany, Atmos. Environ., 34, 3779–3788, doi:10.1016/s1352-2310(99)00518-x, 2000.

Szidat, S., Jenk, T. M., Synal, H. A., Kalberer, M., Wacker, L., Hajdas, I., Kasper-Giebl, A., and Baltensperger, U.: Contributions of fossil fuel, biomass-burning, and biogenic emissions to carbonaceous aerosols in Zurich as traced by C-14, J. Geophys. Res.-Atmos., 111, D07206, doi:10.1029/2005jd006590, 2006.

Szidat, S., Ruff, M., Perron, N., Wacker, L., Synal, H.-A., Hallquist, M., Shannigrahi, A. S., Yttri, K. E., Dye, C., and Simpson, D.: Fossil and non-fossil sources of organic carbon (OC) and elemental carbon (EC) in Göteborg, Sweden, Atmos. Chem. Phys., 9, 1521–1535, doi:10.5194/acp-9-1521-2009, 2009.

Szmigielski, R., Surratt, J. D., Gomez-Gonzalez, Y., Van der Veken, P., Kourtchev, I., Vermeylen, R., Blockhuys, F., Jaoui, M., Kleindienst, T. E., Lewandowski, M., Offenberg, J. H., Edney, E. O., Seinfeld, J. H., Maenhaut, W., and Claeys, M.: 3-methyl-1,2,3-butanetricarboxylic acid: an atmospheric tracer for terpene secondary organic aerosol, Geophys. Res. Lett., 34, L24811, doi:10.1029/2007gl031338, 2007.

Tritscher, T., Dommen, J., DeCarlo, P. F., Gysel, M., Barmet, P. B., Praplan, A. P., Weingartner, E., Prévôt, A. S. H., Riipinen, I., Donahue, N. M., and Baltensperger, U.: Volatility and

ACPD
12, 20311–20350, 2012

hygroscopicity of aging secondary organic aerosol in a smog chamber, Atmos. Chem. Phys., 11, 11477–11496, doi:10.5194/acp-11-11477-2011, 2011.

Tsimpidi, A. P., Karydis, V. A., Zavala, M., Lei, W., Bei, N., Molina, L., and Pandis, S. N.: Sources and production of organic aerosol in Mexico City: insights from the combination of a chemical transport model (PMCAMx-2008) and measurements during MILAGRO, Atmos. Chem. Phys., 11, 5153–5168, doi:10.5194/acp-11-5153-2011, 2011.

Virtanen, A., Joutsensaari, J., Koop, T., Kannosto, J., Yli-Pirila, P., Leskinen, J., Makela, J. M., Holopainen, J. K., Poschl, U., Kulmala, M., Worsnop, D. R., and Laaksonen, A.: An amorphous solid state of biogenic secondary organic aerosol particles, Nature, 467, 824–827, doi:10.1038/nature09455, 2010.

Volkamer, R., Jimenez, J. L., San Martini, F., Dzepina, K., Zhang, Q., Salcedo, D., Molina, L. T., Worsnop, D. R., and Molina, M. J.: Secondary organic aerosol formation from anthropogenic air pollution: rapid and higher than expected, Geophys. Res. Lett., 33, L17811, doi:10.1029/2006gl026899, 2006.

Yasmeen, F., Vermeylen, R., Szmigielski, R., Iinuma, Y., Böge, O., Herrmann, H., Maenhaut, W., and Claeys, M.: Terpenylic acid and related compounds: precursors for dimers in secondary organic aerosol from the ozonolysis of α- and β-pinene, Atmos. Chem. Phys., 10, 9383–9392, doi:10.5194/acp-10-9383-2010, 2010.

Zhang, Y. Y., Müller, L., Winterhalter, R., Moortgat, G. K., Hoffmann, T., and Pöschl, U.: Seasonal cycle and temperature dependence of pinene oxidation products, dicarboxylic acids and nitrophenols in fine and coarse air particulate matter, Atmos. Chem. Phys., 10, 7859–7873, doi:10.5194/acp-10-7859-2010, 2010.

Zobrist, B., Marcolli, C., Pedernera, D. A., and Koop, T.: Do atmospheric aerosols form glasses?, Atmos. Chem. Phys., 8, 5221–5244, doi:10.5194/acp-8-5221-2008, 2008.

ACPD
12, 20311–20350, 2012

Table 1. Summary of SOA mass yields of aromatic compounds included in this study. High and low NO_x refers to 10 ppb and 1 ppb respectively. Given are also the respective OH rate coefficients from the NIST Kinetic Data Base. For comparison are the OH reaction rate coefficients of the monoterpenes $k_{\alpha\text{-pinene+OH}} = 5.3 \times 10^{-11}$ and $k_{\text{limonene+OH}} = 1.6 \times 10^{-10}\,\text{cm}^3\,\text{s}^{-1}$. C_{OA} provides the organic aerosol mass concentration at the end of the experiment, corrected for flush out and wall deposition.

Experiment	AVOC	NO_x	Rate coefficient ($cm^3\,s^{-1}$)	SOA Yield	C_{OA} ($\mu g\,m^{-3}$)
ASOA (8/6)	benzene	high	1.2×10^{-12}	0.031	1.4
ASOA (7/6)	benzene	low	1.2×10^{-12}	0.082	5.9
ASOA (1/8)	benzene	low	1.2×10^{-12}	0.0005	0.03
ASOA (4/8)	toluene	low	5.6×10^{-12}	0.002	0.18
ASOA (11/6)	toluene	low	5.6×10^{-12}	0.039	1.9
ASOA (14/6)	p-xylene	low	1.4×10^{-11}	0.012	0.48
ASOA (16/6)	p-xylene	high	1.4×10^{-11}	0.042	2.5
ASOA (21/7)	p-xylene	low	1.4×10^{-11}	0.018	0.5
ASOA (16/8)	p-xylene (D_{10})	low	($\approx 1.4 \times 10^{-11}$)[1]	0.0007	0.019
ASOA (21/7)	p-cymene	high/NO_2	1.51×10^{-11}	0.045	2.5
ASOA (22/7)	p-cymene	high/NO	1.51×10^{-11}	0.091	5.4
ASOA (25/7)	p-cymene	low	1.51×10^{-11}	0.021	0.78
ASOA (21/6)	mesitylene	high	5.67×10^{-11}	0.021	0.3
ASOA (17/6)	mesitylene	low	5.67×10^{-11}	0.027	0.4
ASOA (10/8)	mesitylene	low	5.67×10^{-11}	0.0004	0.01
ASOA (27/7)	HMB[2]	low	1×10^{-10}[3]	0.0001	0.018
ASOA (29/7)	HMB[2]	low	1×10^{-10}[3]	0.0001	0.019

[1] estimated from p-xylene.
[2] hexamethylbenzene.
[3] Berndt and Böge (2001).

ACPD
12, 20311–20350, 2012

Table 2. Summary of initial precursor concentrations and selected quantities at the time of filter collection. The OH dose is the accumulated measured dose since BVOC and AVOC addition, respectively. All uncertainties given are the statistical standard deviations. The ASOA fraction is estimated by model calculations and derived from f44 observed in ASOA and BSOA by AMS.

Experiment	BVOC precursor (ppb)	AVOC precursor (ppb)	SOA mass ($\mu g\,m^{-3}$) ± stdev	OH-dose AVOC ($cm^{-3}\,s$)	OH-dose BVOC ($cm^{-3}\,s$)	VFR_{343K}	O/C ± stdev	ASOA fraction[1] (%)
ABSOA (10/6)	α-pinene & limonene (40 ppb)	toluene (85 ppb)	16.4 ± 1.5	1.6×10^{10}	3.3×10^{10}	0.86	0.46 ± 0.01	8 (30)
ABSOA (11–12/6)	α-pinene & limonene (40 ppb)	toluene (85 ppb)	14.6[2] ± 0.6	6.5×10^{10}	0.4×10^{10}	0.86	0.43 ± 0.02	8 (9)
ABSOA (14–15/6)	α-pinene & limonene (40 ppb)	xylene (30 ppb)	5.7 ± 0.4	6.7×10^{10}	1.1×10^{10}	0.92	0.45 ± 0.03	13 (18)
ABSOA (22/6)	α-pinene & limonene (8 ppb)	toluene (60 ppb)	3.5 ± 0.4	5.0×10^{10}	5.0×10^{10}	0.94	0.59 ± 0.05	56 (55)
ASOA (11/6)		toluene (85 ppb)	1.2 ± 0.07	6.0×10^{10}	n/a	0.98	0.36 ± 0.12	100
ASOA (13/6)		toluene (85 ppb)	4.7 ± 0.4	8.5×10^{10}	n/a	0.98	0.79 ± 0.04	100
ASOA (14/6)		xylene (30 ppb)	0.20 ± 0.03	5.6×10^{10}	n/a	0.95	0.44 ± 0.22	100
BSOA[3] (18/6)	α-pinene (40 ppb)		26.2 ± 1.6	n/a	2.1×10^{10}	0.79	0.43 ± 0.02	0
BSOA[3] (19/6)	α-pinene (40 ppb)		6.4 ± 0.2	n/a	6.0×10^{10}	0.88[4]	0.46 ± 0.02	0

[1] Values in () from AMS measurements.
[2] longer SOA lifetime due to failure of mixing fan.
[3] Salo et al. (2011), ACP.
[4] 2 h after filter.

ACPD
12, 20311–20350, 2012

Table 3. Concentration of quantified BSOA tracer compounds in filter samples. All listed compounds were below detection limit (b.d.) in ASOA samples (11/6 and 13/6). Concentration in ng m^{-3} if not stated elsewise. Molecular weights MW are given in g mol^{-1}.

Compound name, abbreviation and MW	ABSOA (10/6)	ABSOA (12/6)	ABSOA (15/6)	ABSOA (22/6)	BSOA (18/6)	BSOA (19/6)
Terpenylic acid (TPA) MW = 172	28.7	28.6	11.1	10.9	76.6	11.6
Diaterpenylic acid acetate (DTAA) MW = 232	6.9	3.7	2.0	2.8	25.3	5.2
Pinic acid (AP1) MW = 186	63.9	69.2	17.2	12.7	613.5	36.3
cis-pinonic acid (AP2) MW = 184	3.0	3.7	1.5	2.9	13.8	1.9
Hydroxy-pinonic acid[2] (AP3) MW = 200	15.2	35.1	4.9	3.6	21.1	9.7
Norlimonic acid[1] (Li1) MW = 186	34.3	39.8	7.2	2.4	b.d	b.d
Keto-limononic acid[2] (Li2) MW = 186	7.9	19.5	11.8	1.3	b.d	b.d
Keto-limonic acid[1] (Li3) MW = 188	188.7	158.1	20	9.4		
Hydroxy-keto-limononic acid[1] (Li4) MW = 202	145.0	121.7	30.1	17.1		
unknown acid[1] MW = 188					97.2	9.8
unknown acid[1] MW = 202					111.6	13.5
Sum of 1. generation products						
[ng m^{-3} air]	493.6	479.4	105.8	63.1	59.1	88
[ng µg^{-1} PM]	30.1	32.8	18.6	18.0	36.6	13.8
2. generation product 3-Methyl butane tricarboxylic acid (3-MBTCA) MW = 204						
[ng m^{-3} air]	4.1	4.4	4.8	30.2	320.8	42.7
[ng µg^{-1} PM]	0.3	0.3	0.8	8.6	12.2	6.7
Terpenyl-diaterpenyl dimer ester[3] (DE1) MW = 344	0.7			0.7	18.3	1.8
Pinyl-diaterpenyl dimer ester[3] (DE2) MW = 358	7.3	2.5	1.0	5.2	292.5	28.6
Pinonyl-pinyl dimer ester[2] (DE3) MW = 368	7.4	3.5	1.4	1.4	141.8	11.5
Sum dimer esters						
[ng m^{-3} air]	15.4	6	2.4	7.3	452.6	41.9
[ng µg^{-1} PM]	0.9	0.4	0.4	2.1	17.3	6.5

[1] Quantified using *cis*-pinic acid as surrogate standard.

[2] Quantified using *cis*-pinonic acid as surrogate standard.

[3] Quantified using averaged standard curves of the precursors (see Kristensen et al., 2012).

ACPD
12, 20311–20350, 2012

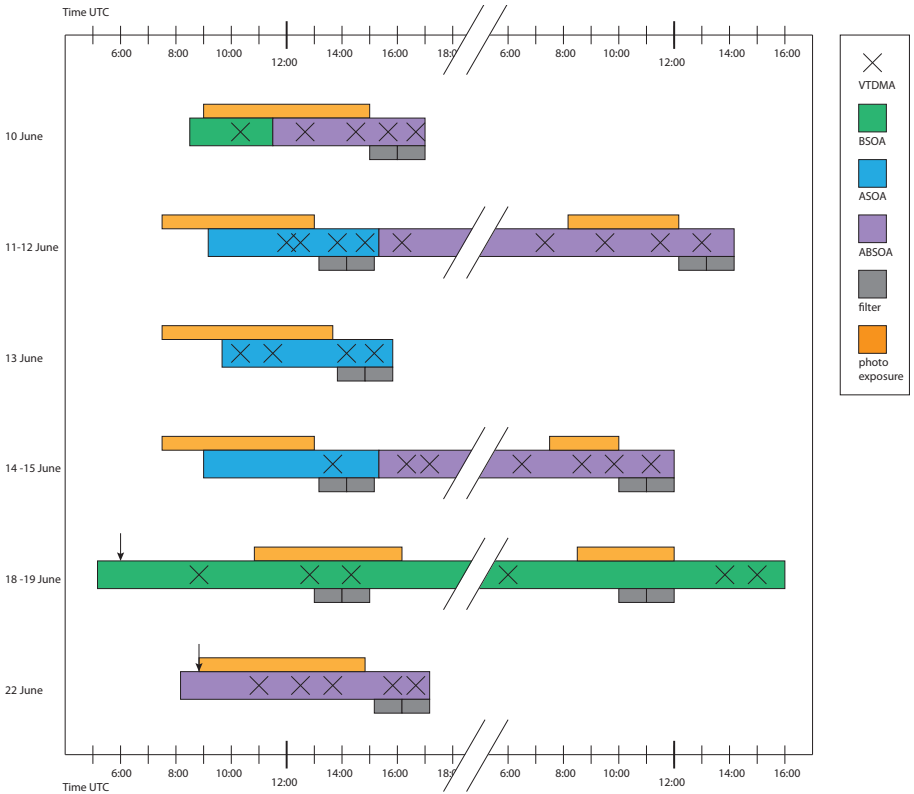

Fig. 1. An overview of the experimental procedures. Main bars indicate SOA-type; ASOA (blue), BSOA (green), and ABSOA (violet). Sunlight exposure is shown by orange bars and filter sampling by grey. Crosses indicate measurements VFR_{343K} by VTDMA. The arrows indicate when extra ozone was added to the chamber. Before experiment 11-13/6, 13/6 and 14/6 the SAPHIR chamber was exposed to sunlight before addition of organic precursor in order to determine the background reactivity.

ACPD
12, 20311–20350, 2012

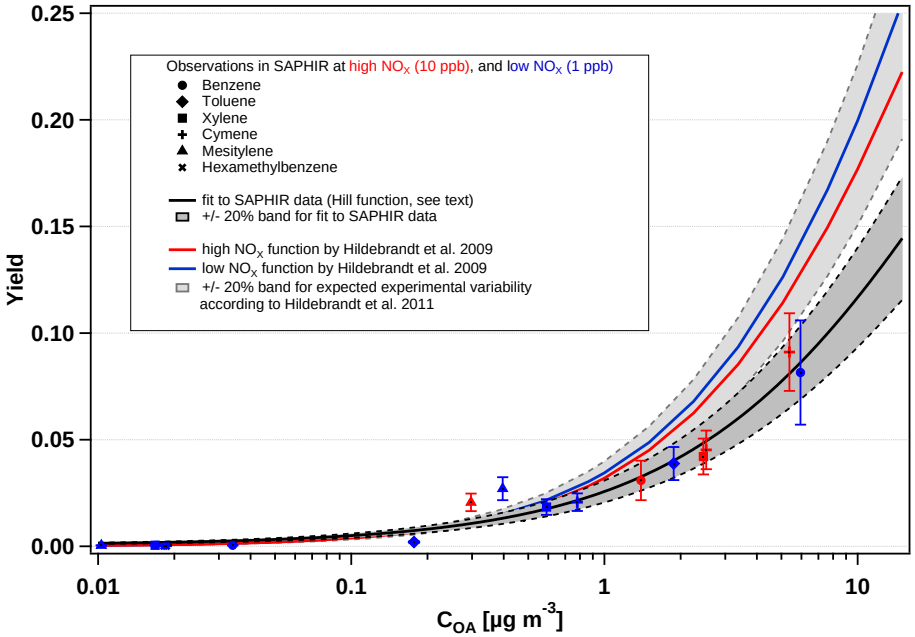

Fig. 2. ASOA mass yield as a function of the organic aerosol concentration for aromatic (anthropogenic) precursors and cymene. The data points and the black fitting curve were achieved in this study. The blue and red curves were calculated according to Hildebrandt et al. (2009). Bands of ±20 % uncertainty intervals are grey shaded. We acknowledge the kind support by Lea Hildebrandt.

ACPD
12, 20311–20350, 2012

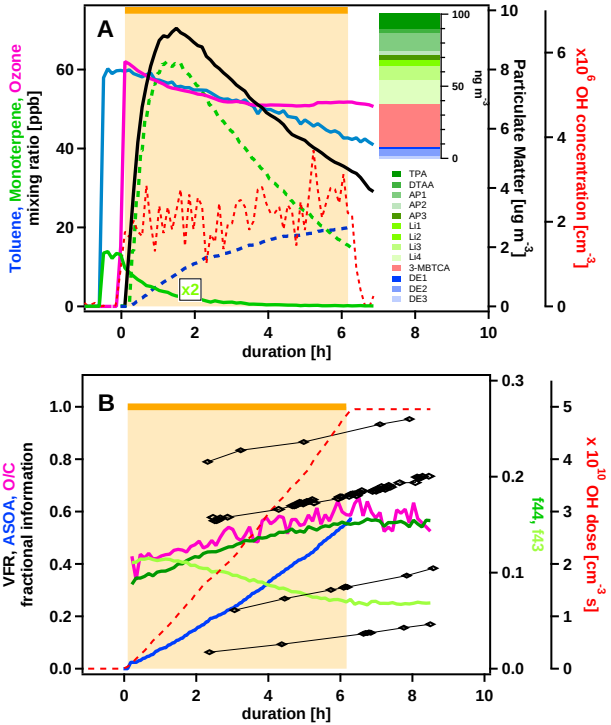

Fig. 3. ABSOA experiment 22/6 where biogenic and anthropogenic precursors are added simultaneously. Top panel **(A)** shows the concentrations of reactants toluene (blue), monoterpenes (green), ozone (magenta), OH (red dashed) and produced SOA (black). The model derived biogenic (green) and anthropogenic (blue) SOA fractions are given as dashed lines. The inset shows the results of the filter analysis at the end of the experiment (compare Table 3). Bottom panel **(B)** shows the aerosol particle properties VFR_{343K}, VFR_{373K}, VFR_{423K}, VFR_{463K} (black diamonds), O/C (magenta), f44 (dark green), and f43 (light green) together with model derived anthropogenic aerosol fraction (blue) and the OH dose (red dashed).

ACPD
12, 20311–20350, 2012

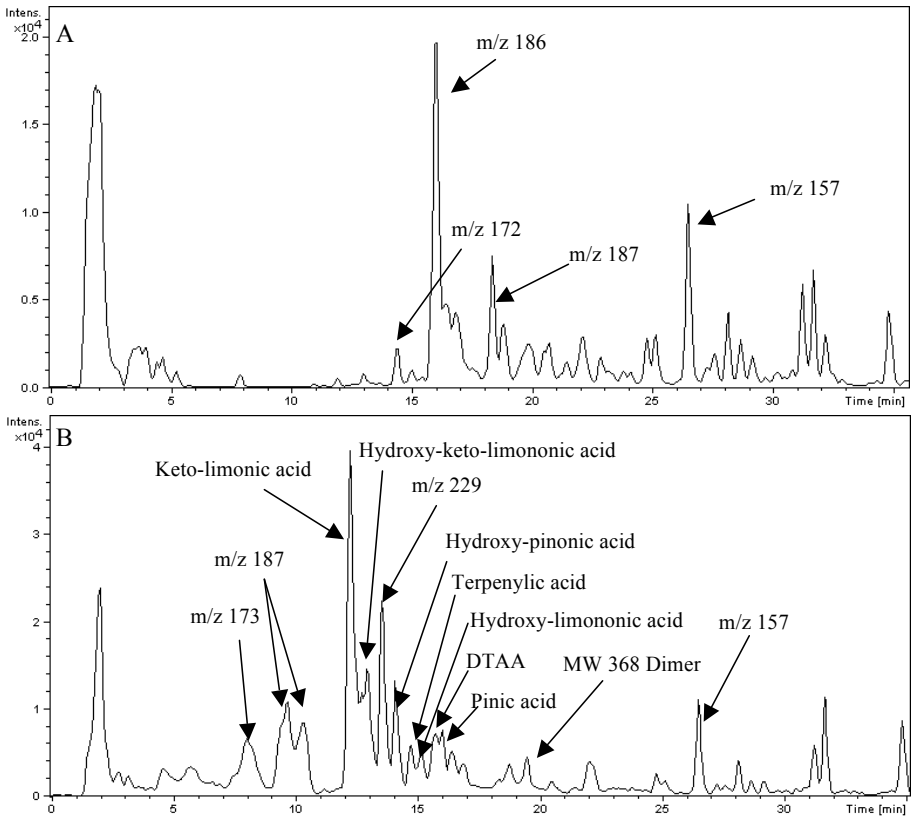

Fig. 4. Total ion chromatogram of organic acids in aerosols from **(A)** toluene after ageing (exp. 11/6), and **(B)** the same experiment after addition of BVOC mix and further ageing (exp. 12/6). Major identified and unidentified peaks are highlighted.

ACPD
12, 20311–20350, 2012

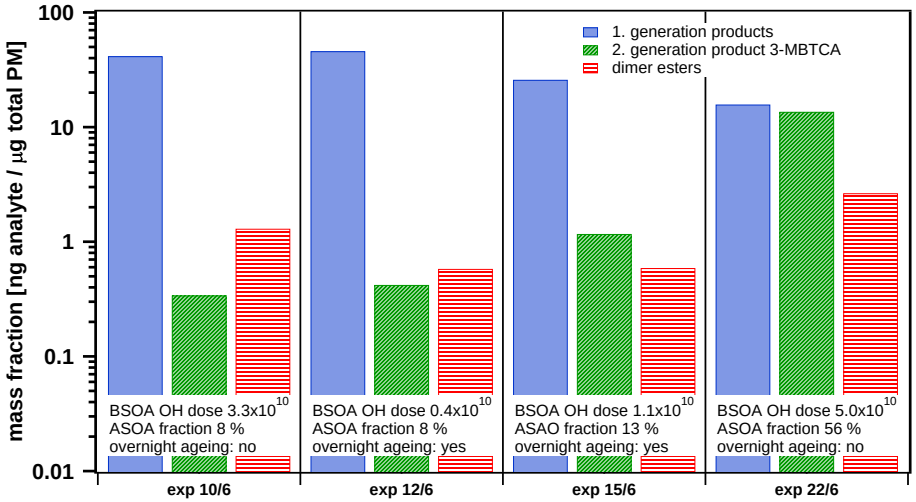

Fig. 5. Relative contribution of first generation products, second generation product 3-MBTCA, and dimer esters to the organic particulate mass. The OH dose seen by the BSOA fraction, the ASOA contribution and the long term ageing are denoted.

ACPD
12, 20311–20350, 2012

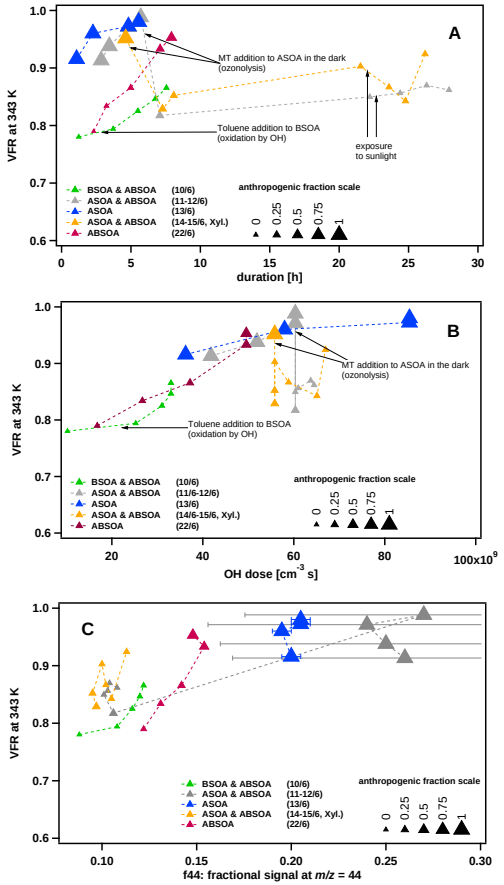

Fig. 6. VFR_{343K} for selected ABSOA experiments as a function of **(A)** elapsed time **(B)** OH dose **(C)** f44. f44 for ASOA 11/26 have a large stdev (grey horizontal error bars) due to low signal compared to ASOA 13/6 (blue horizontal error bars).

ACPD
12, 20311–20350, 2012